Proceedings of the XVII ECSMGE-2019
Geotechnical Engineering foundation of the future
ISBN 978-9935-9436-1-3
© The authors and IGS: All rights reserved, 2019
doi: 10.32075/17ECSMGE-2019-0821

XVII European Conference
ECSMGE 2019
Reykjavik
on Soil Mechanics
and Geotechnical Engineering

Dynamic FE analysis of Soft Boundary (SB) effects on impact pile driving response in centrifuge tests

Analyse par éléments finis dynamiques des effets des limites molles sur la réponse de l'enfoncement des pieux à l'impact lors d'essais de centrifugation

C. X. Azúa-González[a,c], J. C. B. van Zeben[a] , M. Alvarez Grima[b], C. van 't Hof [b] & A. Askarinejad[a]
[a]*Delft University of Technology, Netherlands;* [b] *Royal IHC, Netherlands;* [c]*Cardiff University, UK;*

ABSTRACT: The behaviour of sand and the pile response for impact pile driving has been investigated, both in a series of (dry sand) centrifuge tests and using Finite Elements (FE) in the time domain (on both dry and saturated sand). This study, for the time being, copes with single hammer blow effects and the FE technique is restricted to small deformation analysis. Centrifuge tests with open-ended piles are being carried out using a small-beam centrifuge at Delft University of Technology (DUT), where space limitations are present. Therefore, potential boundary effects have been studied numerically. In this regard, blinded predictions have been performed to evaluate the use of lateral Soft Boundaries (SB) as a potential mitigation strategy for boundary effects in the experimental setup. Relative densities have been considered in the range of 30 % to 90 % for loose and dense sand, respectively. In the absense of experimental data on saturated conditions, both drained and undrained cases have been considered to study, numerically, the hydro-mechanical response of soil during and after the application of a single hammer blow. A hypoplastic law for soils has been used, while soil-structure interaction has been addressed using a continuum-based interface. Validation of numerical findings on dry sand have been carried out using preliminary experimental results. Blinded numerical simulations have shown lateral SB may attenuate boundary effects for a single hammer blow in saturated sand, however, an experimental campaign is still needed.

RÉSUMÉ: Le comportement du sable et la réponse du tas de sable pour le battage de pieux à l'impact ont été étudiés, à la fois dans une série d'essais de centrifugation (sable sec) et en utilisant des éléments finis (EF) dans le domaine temporel (sur sable sec et saturé). Cette étude, pour l'instant, tient compte des effets de coup de marteau unique et la technique EF est limitée à de petites analyses de déformation. Des essais de centrifugation avec des pieux ouverts sont effectués à l'aide d'une centrifugeuse à petits faisceaux à l'Université technique de Delft , où l'espace est limité. Par conséquent, les effets limites potentiels ont été étudiés numériquement. À cet égard, des prédictions à l'aveugle ont été effectuées pour évaluer l'utilisation des limites molles latérales (SB) comme stratégie d'atténuation potentielle des effets de limite dans le cadre expérimental. Les densités relatives ont été considérées dans une fourchette de 30 % à 90 % pour le sable meuble et pour le sable dense, respectivement. En l'absence de données expérimentales sur les conditions saturées, les cas drainés et non drainés ont été considérés pour étudier, numériquement, la réponse hydro-mécanique du sol pendant et après l'application d'un seul coup de marteau. Une loi hypoplastique pour les sols a été utilisée, tandis que l'interaction sol-structure a été traitée à l'aide d'une interface basée sur un continuum. La validation des résultats numériques sur sable sec a été effectuée à partir de résultats expérimentaux préliminaires. Des simulations numériques en aveugle ont montré que le limites molles latérales peut atténuer les effets de limite pour un seul coup de marteau dans du sable saturé, cependant, une campagne expérimentale est encore nécessaire.

Keywords: Pile driving; Finite Elements; geo-centrifuge; soil-structure interaction; boundary effects

1 INTRODUCTION

Centrifuge testing is a widespread physical modelling technique in Geotechnical Engineering, which aims to study system response in reduced-scale models. Due to the centrifuge-induced local acceleration, stresses are reproduced as in full scale conditions if appropriate scaling laws are considered (Garnier et al. 2007). Therefore, geo-centrifuge modelling offers the possibility to investigate the response of foundation systems through tests under different boundary conditions without venturing in costly full scale tests.

Nevertheless, mechanical boundaries may influence on the system response when space limitations are present in the experimental facilities. This is the case of the small-beam centrifuge at Delft University of Technology (DUT) (Allersma 1994); and similar space restrictions may be faced at other facilities. Under these circumstances, special attention needs to be given to boundary effects, and mitigation strategies in case they are prone to occur.

In the literature, various methodologies have been proposed to investigate and potentially correct mechanical boundary effects in Geotechnical Engineering. The reader may refer to Pozo (2016) for a brief review on available methods to alleviate boundary effects.

In this paper, the influence of boundary effects on the behaviour of sand and pile response in a series of impact pile driving centrifuge tests has been investigated through numerical predictions using a Finite Elements (FE) approach in the time domain. This study, for the time being, copes with single hammer blow effects and the FE technique is restricted to small deformation analysis. Available driving experiments correspond to tests on open-ended piles, which were performed on dry sand only (for the time being). The FE software package PLAXIS (Brinkgreve et al. 2016) has been used. Numerical simulations cope with both dry and saturated sand, however, predictions have been compared against an experiment on dry sand only (for the time being). Multiple hammer blow effects are yet to studied, where the use of a large deformation FE technique is desirable.

Variables are presented at centrifuge scale (as used in simulations), unless otherwise stated by considering appropriate scaling laws. Soil Mechanics sign convention has been adopted.

2 PHYSICAL MODELLING

2.1 Soil characteristics

Geba sand has been chosen for the centrifuge tests. It is a uniform silica sand which consists of rounded to sub-angular particles with a mean grain size d_{50} of 0.12 mm (De Jager et al. 2017). The sand has a mean uniformity coefficient c_u of 1.46 and a curvature coefficient c_c of 1.15. The minimum and maximum void ratio ($e_{\min}$ and $e_{\max}$) were determined to be 0.64 and 1.07, respectively. The mean specific gravity of the sand G_s was found to be 2.67.

Soil packing state is hereafter referred in terms of the Relative Density $RD = 100 \cdot (e_{\max} - e_0) / (e_{\max} - e_{\min}) [\%]$, where e_0 is the initial void ratio.

2.2 Experimental setup

Centrifuge devices have been designed by van Zeben et al. (2018) including a high-density polyethylene (HDPE) cylindrical container of internal diameter $D_{\text{box,int}}$ = 29.5 cm, an electro-mechanical pile hammering device, a ram-anvil-pile system, and a simple pile guiding system. The pile was manufactured from a steel pipe with an external diameter D = 4.1 cm, length L = 19 cm and constant thickness ratio D/t = 16.4 along the pile.

A centrifuge experiment has been performed on a pre-embedded pile in dry sand for validation of the numerical model. In this aforementioned

experiment, a ram mass of 0.240 kg was used to ensure a striking velocity as typically observed in impact pile driving ($\approx$ 6 m/s). This test corresponds to a single-blow experiment, where a centrifuge-induced acceleration of $30g$ has been used. The small-scale pile has been pushed until a reasonably large pre-embedment pile length L_{emb} [cm], before the single-blow test was carried out. In this test, the pre-embedment length has been set to $L_{emb} = 0.5L$, and sand specimen depth has been set to H_{sample} = 15 cm. These aforementioned geometrical features were chosen solely to be consistent with geometry of (blinded) numerical predictions on saturated sand which had been already established at the time of centrifuge testing. The soil packing state has been set to RD = 90 %.

Sample preparation has been carried out by a pouring process followed by vibratory compaction to reach the desired soil packing state and mimic soil stress state at rest. A simple sketch of the experimental setup is shown in figure 1.

3 NUMERICAL MODELLING

3.1 FE formulation

Momentum balance for the solid-fluid mixture and fluid transport equations are solved for a volume under the influence of dynamic loads. Under this dynamic loading condition, only fully drained and fully undrained drainage conditions can be currently modelled in PLAXIS.

For the undrained situation, pore pressure increments Δp_w [kPa] are computed directly from the displacement field, i.e. $\Delta p_w = \left(K_w\left(1+e_0\right)/e_0\right)tr\left(\boldsymbol{\varepsilon}\right)$ (only the nodal displacement vector **u** is solved directly), where K_w = 2000 MPa is the water bulk modulus. A cavitation cut-off has been established within a limit suction p_{cav} = 100 kPa to avoid non-physical underpressures to occur.

The mass matrix has been adopted as fully consistent with Galerkin minimization to avoid unnecessary inaccuracies of a lumped scheme.

Rayleigh damping has been used to introduce 0.5 % of damping ratio for the target frequencies f_m [Hz] and f_n [Hz], corresponding to the soil natural frequency (first vibration mode) and the dominant frequency from the input signal (Hashash & Park 2002). This fictitious additional damping aimed to improve convergence only.

The equation of motion has been integrated implicitly using the constant average acceleration method from Newmark (1959) because of its robustness.

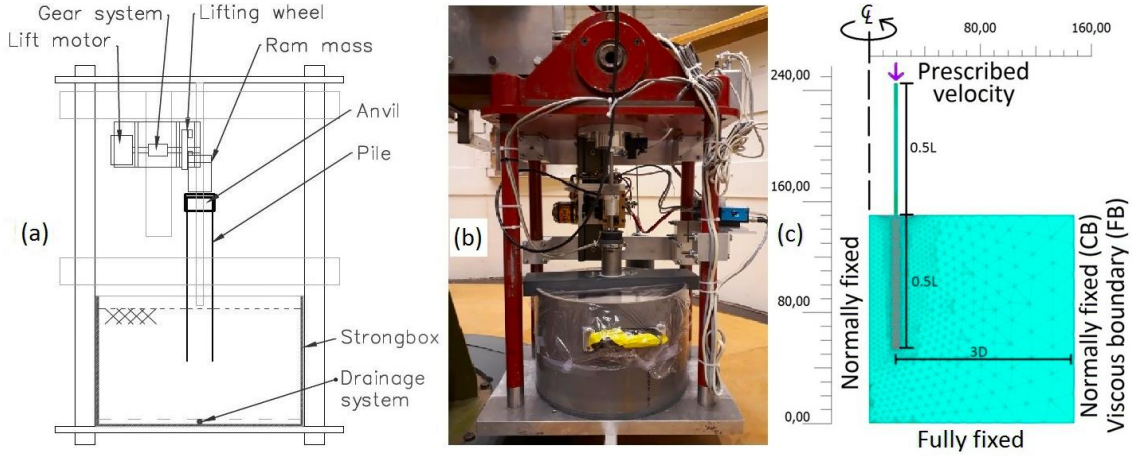

Figure 1. Test setup: a) sketch of components, b) photograph of centrifuge test set up, c) typical axisymmetric FE mesh (RD = 90 %, 3999 elements and 8182 nodes, unit length = 1 mm).

3.2 Simplified FE model

Axisymmetric FE models have been used because of the (pressumed) load symmetry introduced by the pile driving system, i.e. model domain was restricted horizontally to the internal radius of the strongbox ($0.5\,D_{\mathrm{box,int}}$), while soil specimen depth (H_{sample}) was considered vertically. The soil and the pile wall have been modelled by means of 6-noded triangular elements. Soil-structure interaction has been addressed by means of a continuum-based pile-soil interface zone with degraded material properties. For the sake of simplicity, the thickness of this zone t_{deg} has been correlated to the mean grain size. In all the numerical simulations, t_{deg} has been fixed to $10 \cdot d_{50}$. A typical axisymmetric FE mesh was shown in figure 1.

3.2.1 Input signal

A synthetic wavelet was used for the vertical speed of the pile head, to mimic pile strike as

$$v_y = v_{y,peak} \cdot \left(1 - \cos\left[2\pi\left(N/T_{prot}\right)t\right]\right) \quad \text{[m/s]}$$

for $t \in \left(0, T_{prot}/N\right)$ [s], where $v_{y,peak}$ [m/s] is the peak striking speed, T_{prot} [s] is the dwell time at prototype scale (time needed for the impact energy to be transferred from ram mass to anvil-pile system at full scale) and N indicates how many times the centrifuge-induced local gravity has been increased with respect to g = 9.81 m/s^2 (N = 30 has been used in all simulations).

The dwell time has been set to T_{prot} = 10^{-3} s. This value lies in the typical range observed in full scale pile driving ($\approx 10^{-3}$ s to $2 \cdot 10^{-3}$ s).

A frequency upper bound $f_n \approx 200 \cdot N$ [Hz] was reasonably set for a range of typical centrifuge accelerations ($30g$ to $50g$) based on Fourier analysis.

3.3 Boundary Conditions (BC)

Two types of BC were used, i.e. Constrained Boundaries (CB) to mimic the experimental situation and Free-field Boundaries (FB) to mimic the lateral Soft Boundary situation.

3.3.1 Constrained Boundaries (CB)

Lateral and bottom BC have been set to normally fixed and fully fixed, respectively.

3.3.2 Free-field Boundaries (FB)

In future experiments, Soft Boundaries (SB) such as thin sponge-like rubber might be placed adjacent to lateral container walls to compensate for the large rigidity of strongbox walls. Under dynamic loading, these soft layers would absorb incoming waves. This situation has been simulated via virtual SB using distributed dashpots (Lysmer & Kuhlemeyer 1969). In soil dynamics applications, dashpot coefficients are usually multiplied by correcting factors to cope with angle-dependency. Coefficients as proposed in Amorosi et al. (2010) have been used.

Only lateral SB have been simulated while the bottom boundary has been set to be fully fixed. This choice was undertaken since previous experimental studies (Pozo 2016) have shown that the use of soft layers at bottom boundaries could influence in the response of foundation systems negatively, especially in terms of load-carrying capacity.

3.4 Constitutive laws

3.4.1 Soil

The hypoplasticity model from von Wolffersdorff (1996), later enhanced by Niemunis and Herle (1997) to account for Intergranular Strain (IS) evolution, has been chosen to model the soil. This constitutive law can be expressed in a single tensorial equation as shown in equation 1:

$$\dot{\boldsymbol{\sigma}}'\left(\boldsymbol{\sigma}', e, \hbar, \dot{\boldsymbol{\varepsilon}}\right) = \mathbf{M}\left(\boldsymbol{\sigma}', e, \hbar\right) : \dot{\boldsymbol{\varepsilon}} \qquad (1)$$

Where $\dot{\boldsymbol{\sigma}}^{\circ}$ [kPa] is the Jaumman stress rate tensor; $\mathbf{M}$ [kPa] represents the stiffness; e is the void ratio; $\hbar$ is the IS tensor and $\dot{\boldsymbol{\varepsilon}}$ is the strain rate tensor. This law is rate-independent and incrementally non-linear in $\dot{\boldsymbol{\varepsilon}}$.

The basic hypoplasticity law requires eight model parameters, and five added parameters are required to incorporate the IS concept.

These two parameter sets have been previously calibrated based on laboratory tests on Geba sand (Mašin 2017). Soil hypoplastic parameters have been adjusted to account for material degradation in the pile-soil interface zone. A rough pile-soil interface was attempted by adjusting the basic parameter set until shear strength and stiffness were reduced into $\approx 2/3$ of its original response in Direct Shear (DS) experiments. Parameters for Geba sand are shown in table 1.

Table 1. Parameter set: 1) soil, 2) pile-soil

Von Wolffersdorff's model parameters								
#	φ'_{cv} [°]	h_s [MPa]	n	α	β	e_{i0}	e_{c0}	e_{d0}
1	34.0	2500	0.3	0.11	2	1.28	1.07	0.64
2	24.2	5500	0.3	0.11	2	1.28	1.07	0.64
IS model parameters								
#		m_R	m_T	R	β_R		χ	
1 & 2		5.5	3.9	10^{-4}	0.3		0.7	

3.4.2 Pile

Pile wall has been modelled as a Linear Elastic (LE) material. Elastic constants correspond to material properties of steel, i.e. Young's modulus E_{st} = $2 \cdot 10^5$ MPa and Poisson's ratio ν_{st} = 0.3.

3.5 FE mesh and time discretization

FE discretization has been set to properly trace wave propagation. Element size in the near field l_{nf} [cm] has been set to one-tenth of the average shear-wavelength $\lambda_s = v_s / f_n$ [cm] (as expected adjacent to pile wall), where v_s [m/s] is the shear wave velocity, and f_n [Hz] is the frequency upper bound of the input signal. The time step Δt [s] has been set to one-tenth of $\Delta t_{crit} = l_{\min} / v_p$ [s], i.e. the time a P-wave needs to propagate through the smallest element.

3.6 Stress field initialization

Initially, soil stresses have been generated under $1g$ conditions using the so-called k_0 procedure, where the vertical stress σ_{yy} [kPa] balances body forces, and the effective lateral stress is $\sigma'_{xx} = k_0 \sigma'_{yy}$ [kPa] where $k_0 = 1 - \sin(\phi')$.

Subsequently, the stress field due to the centrifuge flight has been simulated by increasing progressively body forces and phreatic pore pressures N times higher in a drained quasi-static calculation phase. Finally, the pile has been simulated as wished in place, by switching soil elements into a LE material with the corresponding properties of steel.

4 NUMERICAL RESULTS

4.1 Blinded predictions on saturated sand

Predictions on saturated sand ($30g$) are discussed below. Both, drained and undrained cases for dense and loose sand (RD = 90 % and 30 %) have been considered.

4.1.1 Influence of virtual SB on soil response

The influence of mechanical boundaries on the behaviour of saturated sand has been analyzed based on the volumetric strain (drained analysis) and pore pressure (undrained analysis) increments. Evolution of these two variables has been studied beneath pile tip and at a horizontal distance of $3 \cdot D$ [cm] with respect to pile tip.

FE predictions showed that oscillations within a regular period may occur due to wave reflections at virtual container walls, under both drained and undrained conditions, while the use of virtual lateral SB conveniently attenuates this effect, see figure 2.

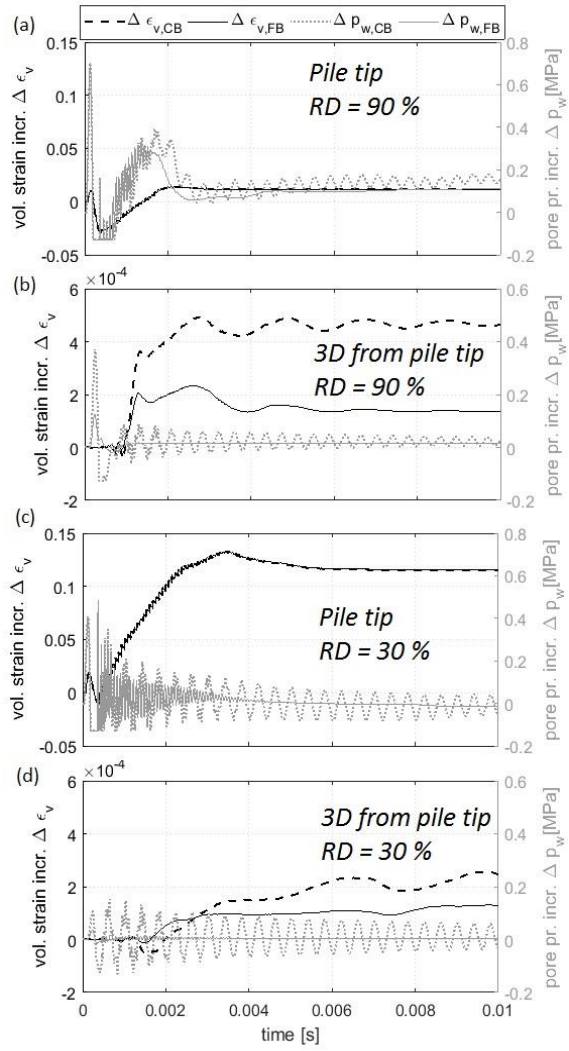

Figure 2. Volumetric strain (drained analysis) and pore pressure (undrained analysis) evolution. Radial distance from pile and relative density as indicated.

Under undrained conditions, pore pressure oscillations at the tip and at a distance of $3 \cdot D$ from this location presented an approximate period equivalent to 9.8 times the travel time of a P-wave along the steel pile in dense sand, which suggests oscillations posses a common period along the radial extension. Here, wave travel time along the pile serves as an artifice for normalization and comparison only. For the drained analysis, volumetric strain oscillations showed similarly a period equivalent to 58 and 85 times the aforementioned travel time in dense and loose sand, respectively. P-wave speeds may be computed approximately taking into account a distance of $6 \cdot D$ and the periods of pore pressure and volumetric strain oscillations to support the idea that radially returning P-waves have a role in boundary effects (strictly speaking waves propagate in different directions not necessarily contained within the horizontal plane). Under undrained conditions, P-wave velocity was estimated between 630 m/s and 682 m/s for loose and dense sand; and 79 m/s and 115 m/s under drained conditions. These backfigured wave speeds may be considered to remain within a credible range for soils (however, yet to be validated more thoroughly via experiments).

4.1.2 Influence of virtual SB on pile response

The influence of mechanical boundaries on pile response has also been analyzed, by means of pile head velocity and displacement in a single hammer-blow test.

Pile head velocity was identified to be least affected between this two measures, since both CB and FB situations showed similar responses as observed in figure 3. This can be explained by the fact that changes in pore pressures (undrained condition) or volumetric strains (drained condition) in the soil were not strong enough to change significantly the immediate pile velocity due to the high inertia contribution of the pile wall (much thicker than for typical open-ended piles, where $D/t \approx 60$ to 100).

Boundary effects could be better identified on residual pile settlement, which evidences the cumulative effect on pile head velocity along the time after a single hammer-blow. Under undrained conditions, boundary effects were predicted to potentially cause over-prediction of pile settlement, however, this is yet to be validated experimentally. In dense sand, the CB case predicted pile settlement in 7.9 % times larger than in the FB case; whereas in 7.4 % for loose sand. This effect on pile settlement in

constrained experiments is thought to be triggered predominantly by reflected P-waves returning to the near field. These reflected waves may pressumably cause significant pore pressure increments in the near field as described in last section; resulting in soil strength and stiffness degradation. On the other hand, when drained conditions have been adopted, boundary effects on pile response were predicted as negligible. The latter may be explained after the small volumetric strain increments ($\approx 10^{-4}$) within soil adjacent to virtual container boundaries, which evidences significant soil constitutive damping in the path between the pile and strobgbox walls.

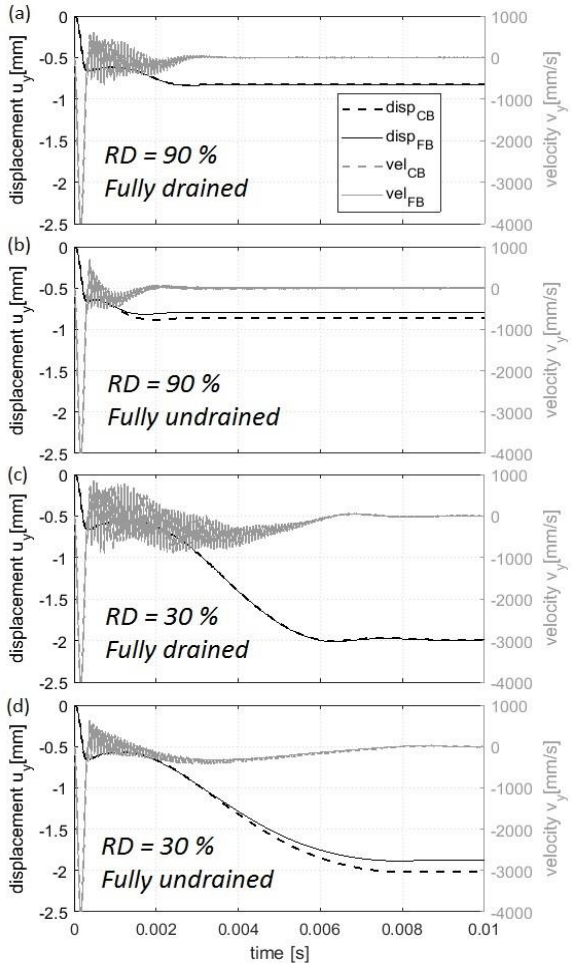

Figure 3. Pile head displacement and velocity time series on FE simulations. Drainage analysis type and relative density (RD) as indicated.

4.2 Validation against experimental data

Pile displacement has been monitored during a single-blow test on dry sand. The peak striking velocity was measured as $v_{y,peak}$ = 4.04 m/s. Time series of pile displacement are shown in figure 4, including a best fit of experimental data (degree 9 polynomial) for comparison against FE predictions (CB and FB cases).

Both numerical predictions showed a similar trend, foreseeing a weak influence of mechanical boundaries in this test. This situation shows the potential of this preliminary centrifuge test on providing insight on the predictive performance of the numerical model. FE predictions were in good agreement in terms of residual pile settlement within an error < 7 %. However, discrepancies were found in terms of local peak displacement amplitude (before rebound) and the time span needed for occurrence of pile rebound.

Numerical simulations underpredicted this aforementioned local peak displacement amplitude and time span by a factor 1.9 and 11.4, respectively. These discrepancies might be attributed to an oversimplification of the energy transfer mechanism (enclosed in a simple velocity wavelet). Other influencing factors may include the inherent soil heterogeneity induced by sample preparation; disregard of anvil inertia effects; and potential deficiencies of the constitutive model calibration within the interface zone (assumed degradation of $\approx 2/3$).

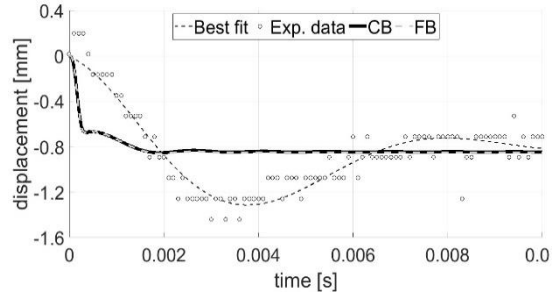

Figure 4. Validation based on pile head displacement.

5 CONCLUSIONS

A numerical investigation has been carried on lateral boundary effects during impact pile

driving centrifuge tests in sand. Blinded predictions on saturated sand suggest boundary effects may disturb pile displacement under undrained conditions. In this case, pile displacement is expected to become slightly larger than for a free-field situation. However, thorough experimental validation on saturated sand is yet to be done.

It has been predicted that the use of lateral SB may be a potential strategy to attenuate boundary effects in these centrifuge experiments.

A validation of numerical predictions on dry sand has been performed. Discrepancies were found between numerical simulations and the validating experimental data; nevertheless, the residual settlement was in good agreement with experimental data. It is recommended that future research focuses on improving the simplified models used in the present work, e.g by accounting for anvil inertia effects. In addition, further analyses should aim to cope with cumulative boundary effects on pile response under repetitive hammer-blows. For this sake, large deformation FE analyses or particle-based techniques are encouraged to be explored.

6 ACKNOWLEDGEMENTS

Financial aid by Royal IHC and additional support by DUT is gratefully acknowledged; the first author appreciates sponsorship by SENESCYT (Ecuadorian Institute for Higher Education). The authors highly appreciate the assistance provided by DUT team of technicians.

7 REFERENCES

Allersma, H. 1994. The University of Delft Geotechnical Centrifuge, *Proc. Int. Conf. Centrifuge 94*, 47–52.

Amorosi, A., Boldini, D., Elia, G. 2010. Parametric study on seismic ground response by finite element modelling, *Comput. Geotech.* **37(4)**, 515–528.

Brinkgreve, R.B.J., Kumarswamy, S., Swolfs, W. 2016. *PLAXIS Manual*, Delft, Netherlands.

De Jager, R., Maghsoudloo, A., Askarinejad, A., Molenkamp, F. 2017. Preliminary results of instrumented laboratory flow slides, *Proc. Engrg.* **175**, 212–219.

Garnier, J., Gaudin, C., Springman, S.M., Culligan, P.J., Goodings, D., Konig, D., Kutter, B., Phillips, R., Randolph, M., Thorel L. 2007. Catalogue of scaling laws and similitude questions in geotechnical centrifuge modelling, *Int. J. Phys. Mod. Geotech.* **7(3)**, 1–23.

Hashash, Y.M., Park, D. 2002. Viscous damping formulation and high frequency motion propagation in nonlinear site response analysis, *Soil Dyn. Eq. Engrg* **22(7)**, 611–624.

Lysmer, J., Kuhlemeyer R.L. 1969. Finite dynamic model for infinite media, *J. Engrg. Mech. Div. (Proc. Am. Soc. Civ. Engr.)* **95(4)**, 859–877.

Mašin, D. 2017. Calibration of sand hypoplastic model on Geba sand data, *Technical report*, Charles University in Prague.

Newmark, N. 1959. A method of computation for structural dynamics, *J. Mech. Div. (Proc. Am. Soc. Civ. Engr.)* **3**, 67–94.

Niemunis, A., Herle, I. 1997. Hypoplastic model for cohesionless soils with elastic strain range, *Mech. Coh. Frict. Mater.* **2(4)**, 279–299.

Pozo, C. 2016. Soft Boundary Effects (SBE) on the behaviour of a shallow foundation, *Master's thesis*, Delft University of Technology, Netherlands.

van Zeben, J.C.B., Azúa-González, C.X., Alvarez Grima, M., van 't Hof, C., Askarinejad, A. 2018. Design and performance of an electro-mechanical pile driving hammer for geo-centrifuge, *Proc. Int. Conf. Phys. Mod. Geotech. (ICPMG 2018)*, 469–473.

von Wolffersdorff, P.A. 1996. A hypoplastic relation for granular materials with a predefined limit state surface. *Mech. Coh. Frict. Mater.* **1(3)**, 251–271.